

# Analyses of Measurements for the First Year of Operation of the Tropical Western Pacific Atmospheric Radiation and Cloud Station

*J. H. Mather and T. P. Ackerman  
Department of Meteorology  
The Pennsylvania State University  
University Park, Pennsylvania*

## Introduction

The first Tropical Western Pacific Atmospheric Radiation and Cloud Station (TWP ARCS) has been operating since October 1996. The TWP ARCS is located on the island of Los Negros, Manus Province, Papua New Guinea, at 2.06°S, 147.42°E. Manus is located in the heart of the western Pacific warm pool region, which is characterized by warm ocean temperatures, high abundances of water vapor, and convective clouds.

The ARCS contains most of the same instruments found at the Southern Great Plains (SGP) Atmospheric Radiation Measurement (ARM) site. The instruments provide a characterization of the surface radiation budget and meteorology along with the vertical distributions of water vapor, temperature, winds, and clouds. A full review of the ARCS can be found in Mather et al. (1998). Presented here are selected data from the first year of operation intended to provide an introduction to the TWP site and to illustrate some of the interesting features that have been observed in the data.

## Surface Meteorology

The high sea surface temperature in the TWP helps to maintain a surface water vapor pressure of 25 hPa to 35 hPa at the ARCS site. The high vapor pressure sets a lower limit on the surface temperature because the air cannot cool below the dew point, which at 25 hPa is equal to 21° C. During the day, the high temperature is moderated by the large heat sink provided by the ocean. The daily minimum temperature usually falls in the range 22° C to 25° C, while the maximum temperature ranges from 28° C to 31° C.

The surface pressure occupies a very narrow range of 1000 hPa to 1015 hPa, although within this narrow range there is a very easily discernible pressure oscillation associated with the semi-diurnal tide. The mean wind speed

for the first year was 3.2 m/s and the wind speed usually fell below 5 m/s. An important exception to the normal light winds occurred during March 1997. A strong (8 m/s to 10 m/s) wind persisted for several weeks. Such westerly wind bursts are thought to signal the onset of El Niño conditions. An associated abstract (Jensen et al. 1998) discusses this westerly wind burst and other phenomena associated with the 1997 El Niño.

## Water Vapor and Surface Radiation

The integrated column water is generally very high in the tropics, rarely dropping below 4 cm. The high abundance of water vapor in the TWP has a huge impact on the downwelling infrared flux at the surface. When the column water vapor is above 4 cm, the 8-micron to 12-micron atmospheric window is nearly opaque. Consequently, clouds have little effect on downwelling infrared (IR) radiation at the surface. Figure 1 (top panel) shows daily averages of the surface downwelling IR radiation plotted against water vapor.

These data show the strong relationship between the downwelling IR and water vapor. They indicate that given the column water vapor, one can estimate the daily averaged downwelling IR to within 10 W/m<sup>2</sup>, regardless of cloud conditions. A linear regression of these data provide the following relationship between water vapor column (WVC, cm) and downwelling IR irradiance at the surface (LW, W/m<sup>2</sup>). Note that this relationship should not be used when the integrated column water is less than 2 cm.

$$LW = WVC * 10.18 + 365.7$$

Figure 1 (bottom panel) demonstrates the correlation between downwelling surface solar radiation and water vapor column. For water vapor column concentrations below approximately 4.5 cm, the daily averaged solar irradiance is nearly constant at 250 W/m<sup>2</sup> to 300 W/m<sup>2</sup>.

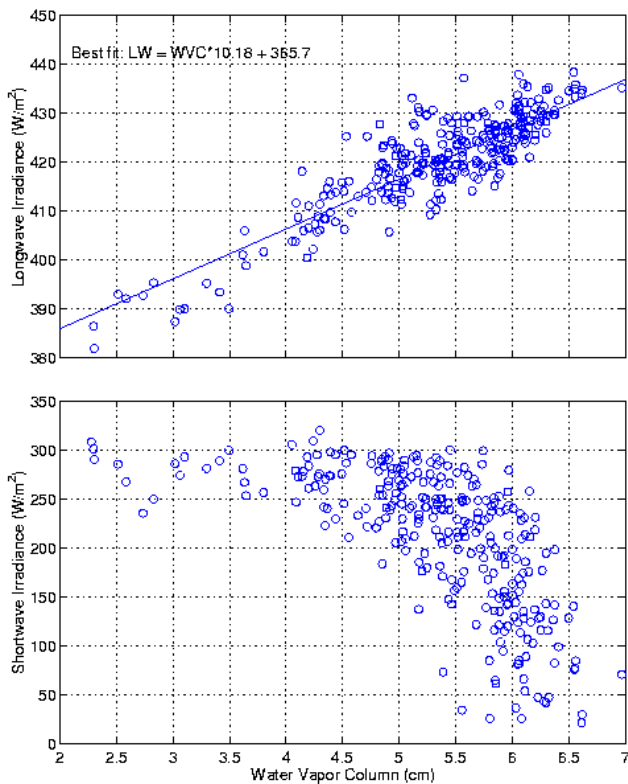


**Figure 1.** Scatter plots of the surface downward longwave (top panel) and shortwave (bottom panel) fluxes versus water vapor column. The data are daily averages for the period October 1996 through August 1997. (For a color version of this figure, please see [http://www.arm.gov/docs/documents/technical/conf\\_9803/mather-98.pdf](http://www.arm.gov/docs/documents/technical/conf_9803/mather-98.pdf).)

These levels of solar radiation correspond to primarily clear-sky conditions and the relatively low column water densities may be due to local subsidence associated with a suppressed convection regime. Above 4.5 cm, the solar irradiance drops sharply indicating a sharp increase in cloud cover. At these higher levels of column water vapor, the relationship between water vapor and shortwave irradiance exhibits a great deal of scatter indicating highly variable cloud cover. This is a regime of active convection. Under these conditions, local upward motion would tend to moisten the column.

Figure 2 shows a 1-year time series of daily averages of shortwave and longwave radiation along with column water vapor. A 10-day running average has been applied to the data. There are several interesting features in this series. The shortwave data in the top panel illustrate a cycle of clear and cloudy periods. For much of the year, the pattern has been a long period of relatively clear conditions

followed by a shorter period of cloudy conditions. There are four such cycles between January and July 1997. The period of these oscillations is approximately 40 days. This corresponds to the period that has been observed for the Madden-Julian oscillation. By comparing the middle and bottom panels in Figure 2, we again see the strong correlation between water vapor and longwave radiation and an anti-correlation between both these series and the shortwave radiation in Figure 2 (top panel).

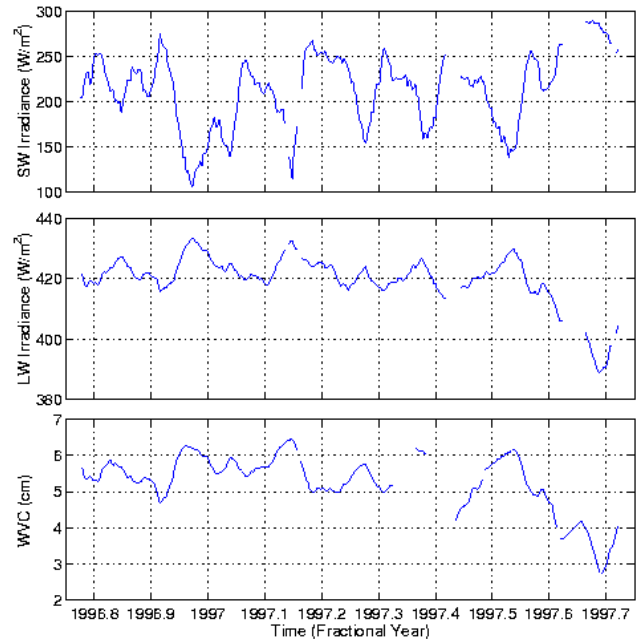


**Figure 2.** Time series of the surface downward shortwave and longwave fluxes and the water vapor column. These data are daily averages with a 10-day running mean applied to filter high frequency variability. (For a color version of this figure, please see [http://www.arm.gov/docs/documents/technical/conf\\_9803/mather-98.pdf](http://www.arm.gov/docs/documents/technical/conf_9803/mather-98.pdf).)

## Clouds and Shortwave Radiation

The frequency of cloud occurrence at the site is obtained with a micropulse lidar (MPL). Figure 3 shows the frequency distribution of cloud base from the MPL for the period February to August 1997. The probability of observing a cloud at any height is 76%. These data exclude a period of approximately 90 minutes about local solar noon (approximately 02 GMT) because the MPL is covered at that time to prevent the front-end optics from focusing the overhead sun onto the detector. The cloud base distribution

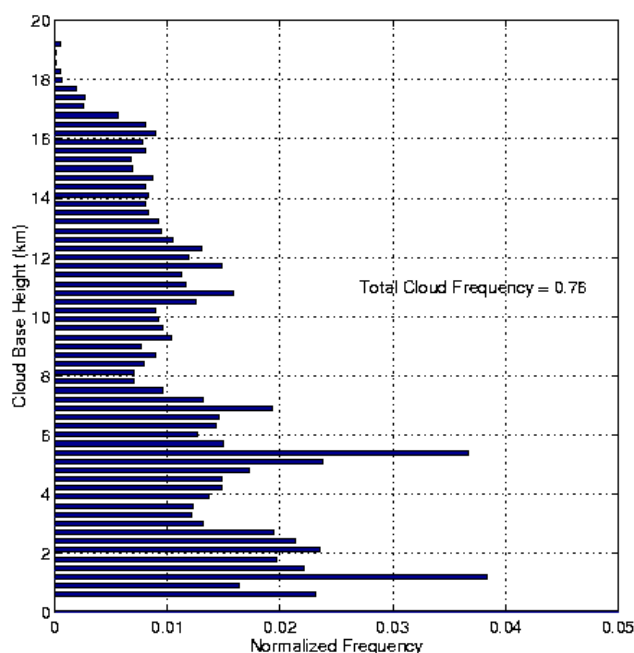


**Figure 3.** Frequency distribution of cloud base height obtained with the MPL. One-minute profiles were used for these statistics and only the lowest cloud base height was used for each profile. Data for this distribution were from the period February to August 1997. (For a color version of this figure, please see [http://www.arm.gov/docs/documents/technical/conf\\_9803/mather-98.pdf](http://www.arm.gov/docs/documents/technical/conf_9803/mather-98.pdf).)

shows an interesting tri-modal distribution with peaks near 2 km, 6 km, and 12 km. Cloud bases are observed up to the tropopause.

To illustrate the effect of clouds on shortwave radiation, we have calculated the normalized shortwave cloud forcing at the surface. Here the shortwave cloud forcing is defined as actual measured downwelling shortwave irradiance minus the irradiance calculated assuming no clouds are present. This difference is normalized by the clear-sky irradiance. Ten-minute averaged data were used for these calculations.

Figure 4 shows normalized cloud forcing data for periods of suppressed and active convection. Ten-minute averaged data from January through July 1997 were used to produce these distributions. The delineation of suppressed and active periods was based on the smoothed surface shortwave radiation data shown in Figure 2 (top panel). We have chosen a threshold of  $200 \text{ W/m}^2$  in the 10-day averaged shortwave as a threshold to separate active and suppressed periods. These data illustrate the cloud forcing patterns and

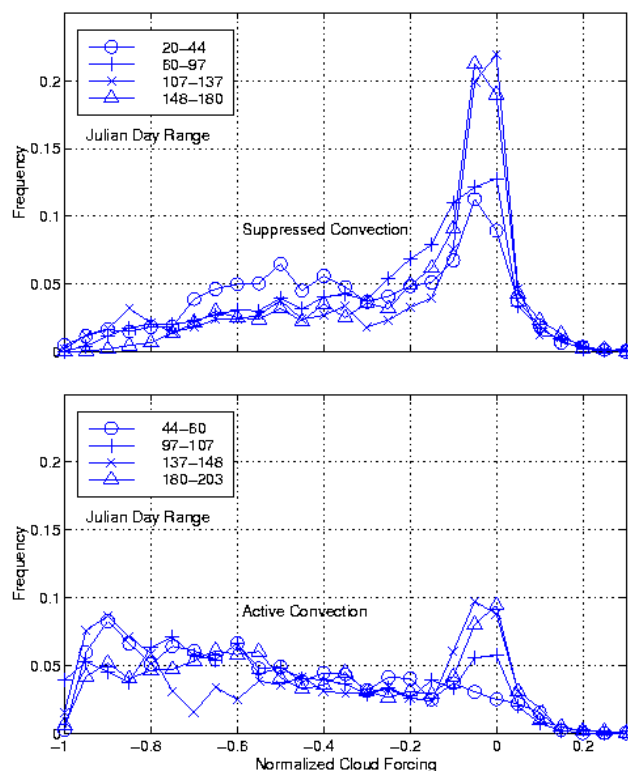


**Figure 4.** Frequency distribution of surface shortwave radiative cloud forcing. The top panel shows the frequency distribution from four periods of suppressed convection, while the bottom panel is from four periods of active convection. Cloud forcing here is defined as (measured shortwave flux – clear-sky flux)/(clear-sky flux). (For a color version of this figure, please see [http://www.arm.gov/docs/documents/technical/conf\\_9803/mather-98.pdf](http://www.arm.gov/docs/documents/technical/conf_9803/mather-98.pdf).)

variability that occur within these broadly defined convective regimes.

Under suppressed conditions, there is a strong peak near zero forcing or clear conditions, although the height of this peak varies by a factor of two among these four cases. The frequency decreases nearly monotonically from a forcing value of -0.1 to -1.0. In the case of active convection, there tends to be a weaker peak near zero cloud forcing with a trend of increasing probability toward strong negative forcing. In both the active and suppressed cases, there are positive cloud forcing events out to approximately 0.2. These positive values correspond to periods when the direct beam is not significantly attenuated and the diffuse field is enhanced by a broken cloud field.

## References

- Jensen, M. P., J. H. Mather, and T. P. Ackerman, 1998: Observations of the 1997-1998 warm-ENSO event at the Manus Island ARM site. This proceedings.
- Mather, J. H., T. P. Ackerman, W. E. Clements, F. J. Barnes, M. D. Ivey, L. D. Hatfield, and R. M. Reynolds, 1998: An atmospheric radiation and cloud station in the tropical western Pacific. *Bull. Amer. Met. Soc.*, **79**, 627-642.